Gelation of fluorinated liquids by non-fluorinated low-molecular-mass molecules†

P. C. Griffiths,*[a] M. Côte,[a] R. James,[a] Ph. G. Rogueda,[b] I. R. Morgan[a] and D. W. Knight[a]

Received (in Cambridge, UK) 29th April 2005, Accepted 30th June 2005
First published as an Advance Article on the web 11th July 2005
DOI: 10.1039/b505938k

A family of tetrahydroxy diesters has been synthesised and observed to gel a range of fluorinated solvents and their mixtures; the phase behaviour and gel microstructure are reported for a homologous family of these diesters in blends of 1*H*,1*H*-heptafluorobutanol (HFB) and 2*H*,3*H*-perfluoropentane (HPFP).

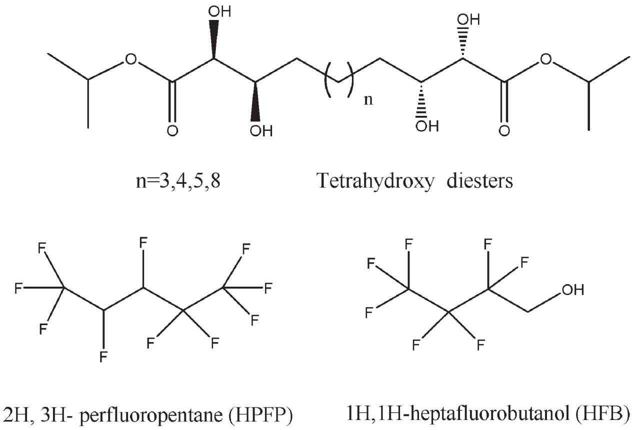

Fig. 1 Structure of the tetrahydroxy diester gelators[11] and fluorinated solvents used in the gelling systems.

Low-molecular-mass organogelators are small molecules that spontaneously self-assemble to create a three-dimensional network capable of entrapping the solvent and creating gels.[1–4] Such systems exhibit great potential for use in the fields of food science, cosmetics and drug delivery.[5–8] Our interest focuses on gels where the entangled phase is a fluorinated solvent. Such solvents are already used as replacement media for blood, liquid ventilation and as contrast agents for ultrasound imaging.[9] However, they need to be formulated with polymers and surfactants in order to introduce the necessary additional physical characteristics. Gelation of fluorinated media has already been reported,[10] using partially fluorinated n-alkanes as the gelling agents. The incompatibility of the fluorocarbon and hydrocarbon segments drives the aggregation of the molecules. However, in this communication we report what we believe to be the first ever gelation of fluorinated solvents by non-fluorinated molecules.

A family of tetrahydroxy diesters was observed to form gels in mixtures of 1*H*,1*H* heptafluorobutanol (HFB) and 2*H*,3*H*-perfluoropentane (HPFP). Fig. 1 presents the structure of both the gelators and fluorinated solvents used in this work. These novel gelators are referred to as G_n, with n = 3, 4, 5 or 8 according to their backbone length.

The synthesis of the gelator involves first a cross metathesis with isopropyl acrylate and the corresponding bis-alkene, using Grubb's second generation catalyst.[12,13] Then, these bis-α,β-unsaturated esters undergo asymmetric dihydroxylation affording the tetrahydroxy gelators in excellent yield and purity.[14] Enantiomeric purity (determined by gas chromatography on a Chiraldex GTA column) and yield obtained were respectively $> 99\%$ and $> 90\%$ (see ESI, Scheme 1† for details of the synthesis).

The tetrahydroxy diesters are soluble in HFB but not in HPFP. Gelation occurs either by first dissolving the gelator in HFB and subsequently adding HPFP, or by the addition of gelator directly to the solvent blend, in a known and controlled solvents ratio. However, gels prepared by adding the gelator directly to the solvent blend were found to be less reproducible. In this work, all gels were obtained by first dissolving the gelator in HFB then subsequently adding HPFP. Provided there is a significantly high gelator concentration, gelation of pure HFB can also be achieved, while this is not the case for pure HPFP. Often gelation requires a heating–cooling cycle,[15] but these present fluorinated gels form spontaneously at room temperature.

A simple measure of gelation has been used to quantify their phase behaviour. The sample must be stable to tube inversion: a gel shows no flow. The macroscopic phase behaviour was found to depend greatly on the solvent ratio, temperature, gelator alkyl chain length (n) and gelator concentration. The phase behaviour of the gelators in two solvent mixtures is presented in Fig. 2. All compositions are expressed as wt%.

Four different macroscopic states are observed which are indicated as Φ_α, Φ_β, Φ_χ and Φ_δ in Figs. 2(a) and 2(b). At the lower concentration of gelator, a clear liquid is observed with a viscosity comparable to that of the pure solvents ($\boldsymbol{\Phi_\alpha}$). With increasing gelator concentration, the sample becomes heterogeneous with agreggates of transparent gel forming within the fluorosolvent blend ($\boldsymbol{\Phi_\beta}$). At higher concentration of gelator, a transparent macroscopically homogeneous gel forms ($\boldsymbol{\Phi_\chi}$). Increasing the gelator concentration further introduces a "haze" to the gel, forming fibrils that may be collected by removal of the solvent, or simply gelator precipitation ($\boldsymbol{\Phi_\delta}$). The kinetics of gel formation also correlates with the appearance of the gels. For highly concentrated gelator systems, the gels form instantaneously. At lower concentrations, gel formation appears to pass through a

---

[a] *School of Chemistry, Main Building, Cardiff University, Cardiff, Wales CF10 3AT. E-mail: griffithspc@cardiff.ac.uk; Fax: +44(0)29 2087 4030; Tel: +44(0)29 2087 5858*
[b] *AstraZeneca R&D Charnwood, Bakewell Road, Loughborough, Leics., UK LE11 5RH. E-mail: philippe.rogueda@astrazeneca.com; Fax: +44(0)15 0964 5555; Tel: +44(0)15 0964 4000*

† Electronic supplementary information (ESI) available: synthesis of the gelators. See http://dx.doi.org/10.1039/b505938k

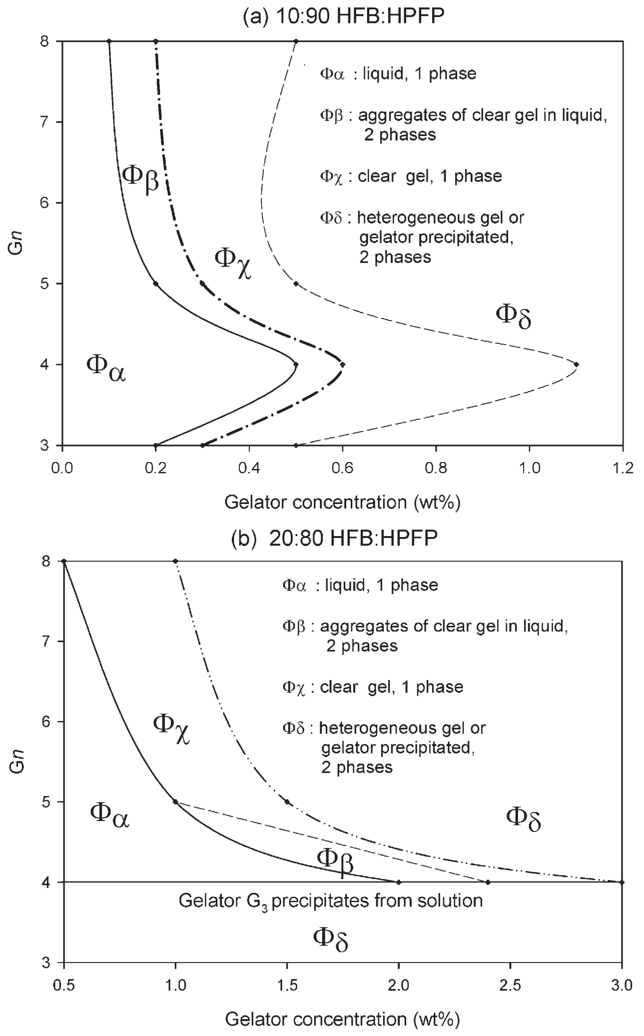

Fig. 2 Macroscopic phase behaviour of G_n for $n = 3, 4, 5, 8$ in (a) 10 : 90 HFB : HPFP and (b) 20 : 80 HFB : HPFP. All gels were made by first dissolving the gelator in HFB then subsequently adding HPFP.

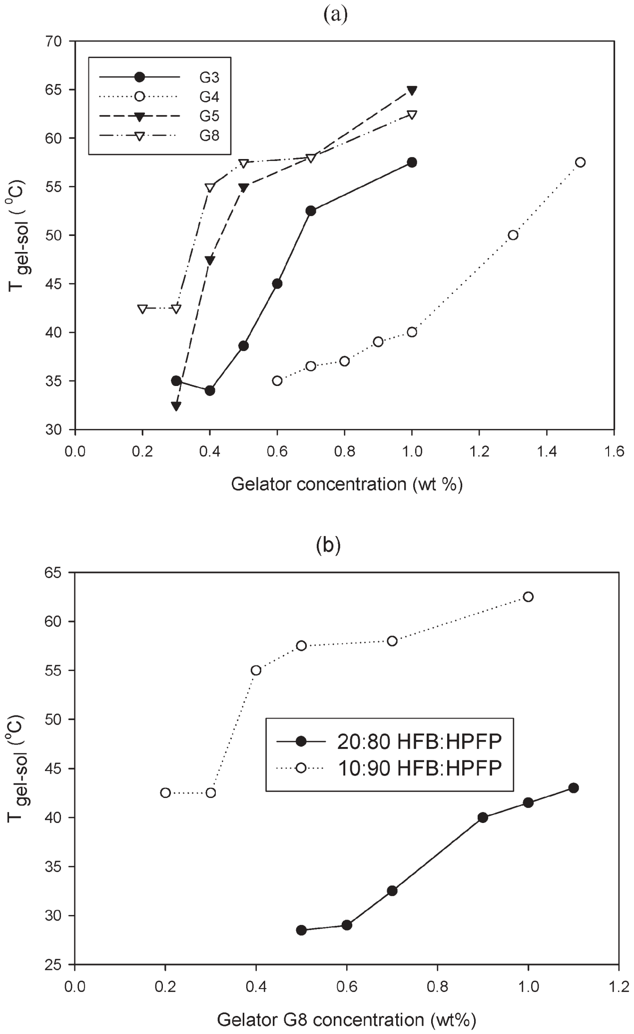

Fig. 3 $T_{\text{gel–sol}}$ for (a) G_3, G_4, G_5, G_8 as a function of G_n concentration in 10 : 90 HFB : HPFP and for (b) G_8 in the two different solvents ratios 10 : 90 and 20 : 80 HFB : HPFP.

growth stage – clear aggregates of gel coexisting with the remaining solvent appear within a few hours, and these coalesce to form a gel throughout the entire sample over a period of days.

For the solvents ratio 10 : 90 HFB : HPFP, from $G_{n\geqslant 4}$, the concentration above which gelation occurs is a decreasing function of increasing *n*: less gelator is required to achieve gelation. For a 10 : 90 HFB : HPFP ratio, transparent fluorinated gels are obtained with the G_8 gelator at a concentration as low as 0.2 wt%, thus G_8 may be considered a supergelator.[16] A deviation is observed for G_3, which requires less gelator than G_4 to obtain an apparently identical gelling behaviour. However, samples made with G_3 were not stable over 3 weeks: the gelator slowly precipitates within the gel.

In the solvent blend 20 : 80 HFB : HPFP, the same general trend is observed, but in this case no gels were formed with gelator G_3. This shows that there is a delicate balance as far as the chain length (*n*) is concerned: decreasing *n* renders this family of gelators less susceptible to self-assembly. Moreover, in the 20 : 80 HFB : HPFP system, a higher concentration of gelator is required to achieve gelation (*i.e.* the phase behaviour is shifted to the right). The same trend is observed for both 30 : 70 and 50 : 50 HFB : HPFP as well as pure HFB. Indeed, HFB acts as the solubilising medium, whereas HPFP, unable to dissolve the gelator, destabilises the initially stable sol.

The gel-to-sol transition temperature ($T_{\text{gel–sol}}$) of the fully gelled samples was measured by immersing the glass vials containing the samples in a temperature controlled waterbath. The temperature at which a sample undergoes a gel to liquid phase transition was noted. $T_{\text{gel–sol}}$ for gelled samples in 10 : 90 HFB : HPFP is presented in Fig. 3(a). A comparison of $T_{\text{gel–sol}}$ obtained for gelator G_8 in 10 : 90 HFB : HPFP and 20 : 80 HFB : HPFP is presented in Fig. 3(b).

It is immediately apparent that, for a given gelator, $T_{\text{gel–sol}}$ increases with increasing gelator concentration and that for samples with the same solvent composition, $T_{\text{gel–sol}}$ increases with the chain length *n*, with the exception of G_3. Then, the same trend is observed in the 20 : 80 HFB : HPFP solvents ratio environment. However, as seen in Fig. 3(b), the $T_{\text{gel–sol}}$ measured are lower than in the 10 : 90 HFB : HPFP ratio, the gelled network requires more gelator to be formed and less energy to be disrupted.

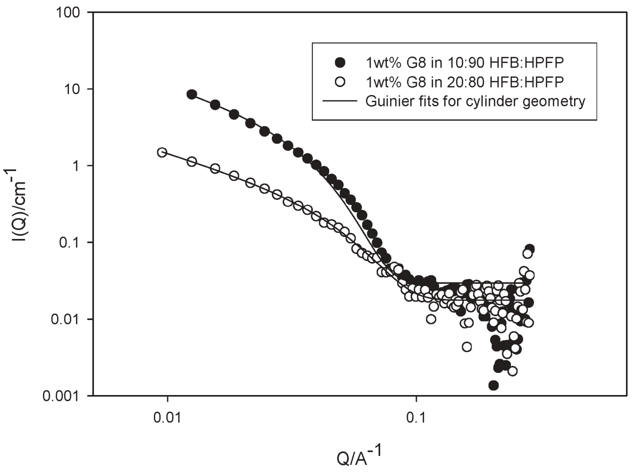

Fig. 4 SANS data obtained for a constant concentration of G_8 in two different HFB : HPFP ratios, along with the Guinier analysis over the low *Q* region for a cylinder geometry (data representative of all the gelled samples investigated with SANS).

To quantify the morphology of the aggregates formed, a preliminary small-angle neutron scattering (SANS) study has been carried out on the LOQ instrument at the ISIS facility, Rutherford Appleton Laboratories, Didcot, UK. Representative data are displayed in Fig. 4.

First, for a given solvent composition, the scattered intensity increases with concentration. For a fixed concentration of gelator, the solvent composition has a pronounced effect on the observed scattering, correlating well with the macroscopic phase behaviour observations. Stronger scattering is observed for gelator G_8 at 1 wt% in a 10 : 90 HFB : HPFP mix than in a 20 : 80 HFB : HPFP, indicating a different packing of the gelator. A Guinier analysis over the low *Q* region of the data – $I(Q) \sim Q^{-1}\exp(-Q^2R^2/4)$ – clearly shows the characteristic signature of a cylinder geometry in the gelled samples, as presented in Fig. 4. The radius (*R*) of the cylinder extracted from the SANS analysis is found to vary both with gelator concentration and solvents ratio. First, for a given solvents ratio, the radius *R* increases with gelator concentration. Let us consider the 50 : 50 HFB : HPFP ratio with gelator G_8. For $G_8 = 3.75$ wt%, $R = 25\ (\pm 1)$ Å, for $G_8 = 5.0$ wt%, $R = 32\ (\pm 1)$ Å and for $G_8 = 6.0$ wt%, $R = 42\ (\pm 1)$ Å. Then, *R* varies according to the solvents ratio. Increasing the proportions of HPFP in the solvents mix results in an increase of *R*. In 100 : 0 HFB : HPFP (*i.e.* pure HFB), $R = 22\ (\pm 1)$ Å, in 50 : 50 HFB : HPFP $R = 30\ (\pm 7)$ Å, in 20 : 80 HFB : HPFP $R = 38\ (\pm 1)$ Å, and finally in 10 : 90 HFB : HPFP $R = 60\ (\pm 1)$ Å, although this behaviour is clearly modulated by the gelator concentration.

Thus the aggregated structures obtained in this gelling process appear to be entangled rod-like fibers that are built up through non-covalent interactions such as weak van der Waals attractions and strong hydrogen-bonding. Freeze-drying one gelled sample clearly shows a swollen structure. The volume of the freeze-dried sample, then constituted only by the entangled fibers of gelators arranged as they were in the original gelled system, is significantly larger than the volume obtained when the gel is left to dry in ambient air. In this last case, as the solvents evaporate, the gelator network collapses. It is not yet absolutely established what forces drive the gelation. These are however likely to be associated with hydrogen bonding in origin since (i) addition of small amounts of water disrupts the gelation[17] and (ii) there is a clear signature in the IR spectra for the presence of hydrogen bonding. This IR signal correlates well with the onset of gelation but not with the sol–gel transition. The band appears when sufficient gelator is present to achieve gelation but does not disappear as a heated gel passes through the gel to sol phase transition. Further work is concentrating on this issue.

We acknowledge financial support from AstraZeneca, the EPSRC and Cardiff University, whilst CCLRC is acknowledged for providing access to the neutron facilities.

Notes and references

1 P. Terech and R. G. Weiss, *Chem. Rev.*, 1997, **97**, 3133.
2 D. J. Abdallah and R. G. Weiss, *J. Braz. Chem. Soc.*, 2000, **11**, 209.
3 O. Gronwald, E. Snip and S. Shinkai, *Curr. Opin. Colloid Interface Sci.*, 2002, **7**, 148.
4 P. Terech, I. Furman and R. G. Weiss, *J. Phys. Chem.*, 1995, **99**, 9558.
5 A. Juteau, N. Cayot, C. Chabanet, J. L. Doublier and E. Guichard, *Trends Food Sci. Technol.*, 2004, **15**, 394.
6 W. B. Davies, Patent Report, *General Pharmacology: the vascular system*, 1993, Vol. **24**, p. xiii.
7 C. Gallegos and J. M. Franco, *Curr. Opin. Colloid Interface Sci.*, 1999, **4**, 288.
8 D. Lichtenberg, P. L. Felgner and T. E. Thompson, *Biochim. Biophys. Acta*, 1982, **684**, 277.
9 J. G. Riess, *Fluorine Chem.*, 2002, **114**, 119; J. G. Riess, *Tetrahedron*, 2002, **58**, 4113; J. G. Riess and M. P. Krafft, *Biomaterials*, 1998, **19**, 1529; M. P. Krafft, A. Chittofrati and J. G. Riess, *Curr. Opin. Colloid Interface Sci.*, 2003, **8**, 251; M. P. Krafft, *Adv. Drug Delivery Rev.*, 2001, **47**, 209.
10 M. George, S. L. Snyder, P. Terech and R. G. Weiss, *Langmuir*, 2005, DOI: 10.1021/la050371z.
11 Work on the synthesis and on the application as catalysts of the tetrahydroxy diesters to be published.
12 A. K. Chatterjee and R. H. Grubbs, *Angew. Chem., Int. Ed.*, 2002, **41**, 3171.
13 S. Randl, S. J. Connon and S. Blechert, *Chem. Commun.*, 2001, 1791.
14 K. B. Sharpless, *J. Org. Chem.*, 1992, **27**, 2768.
15 C. Zhan, P. Gao and M. Liu, *Chem. Commun.*, 2005, 462; G. Clavier, M. Mistry, F. Fages and J. L. Posso, *Tetrahedron Lett.*, 1999, **40**, 9021; H. M. Willemen, T. Vermonden, A. T. M. Marcelis and E. J. R. Sudhölter, *Eur. J. Org. Chem.*, 2001, 2329.
16 A. Valkonen, M. Lahtinen, E. Virtanen, S. Kaikkonen and E. Kolehmainen, *Biosensors Bioelectronics*, 2004, **20**, 1233.
17 S. Tamaru, R. Luboradzki and S. Shinkai, *Chem. Lett.*, 2001, 336.